Proceedings of IMECE 2005:
International Mechanical Engineering Conference and Exposition
November 5-11, 2005, Orlando, Florida

IMECE2005-81672

DESIGN OF A PIEZORESISTIVE SURFACE MICROMACHINED THREE-AXIS FORCE TRANSDUCER FOR MICROASSEMBLY

Gustavo A. Roman
Dept. of Mechanical and Aerospace Engineering
University of Florida, Gainesville, FL

Jessica R. Bronson
Dept. of Mechanical and Aerospace Engineering
University of Florida, Gainesville, FL

Gloria J. Wiens
Dept. of Mechanical & Aerospace Eng.
University of Florida
Gainesville, FL

James F. (Red) Jones
Intelligent Sys. & Robotics Center
Sandia National Laboratories
Albuquerque, NM

James J. Allen
Microsystem Device Technologies
Sandia National Laboratories
Albuquerque, NM

ABSTRACT

One of the challenges facing microrobotic manufacturing is the ability to sense interactions for force-guided assembly of small devices. There is a need for a force transducer with the ability to sense forces in multiple degrees-of-freedom in the mN range with resolution on the order of 10 μN for microassembly applications. This paper presents theoretical studies for developing a surface micromachined piezoresistive force transducer that can measure normal force in the z-direction and moments about the x and y-axes. The devices proposed here are based on a compliant platform design with integrated piezoresistive sensing elements fabricated in a modified SUMMiT process. Various configurations and sensor element layouts are explored to determine the relationship of the applied forces and moments experienced during assembly and the corresponding strain. Structural and finite element analysis is used to determine the elastic response of the device and establish the best locations and orientations of the sensing elements to effectively utilize the piezoresistive effect of the polysilicon sensors. Initial experiments show the polysilicon piezoresistors to have a gauge factor of approximately 25. The expected sensitivities for these devices are presented.

INTRODUCTION

A wealth of research has been conducted in Microelectromechanical Systems (MEMS) technology, but few applications have successfully made it to market. One limiting factor is a lack of reliable microassembly techniques. Some micromachining processes, such as surface and bulk micromachining, yield batch fabricated parts and often do not require post-fabrication assembly steps [1,2]. Other fabrication methods, such as LIGA, do require assembly [3,4]. There are also hybrid microsystems in which components from various fabrication methods must be integrated to create the functioning device [5]. Assembly tasks for parts of this size, from 10-100 microns, require very precise, controlled manipulation in order to produce complex, functional MEMS devices.

A variety of techniques have been developed to facilitate such assembly processes, including the use of microrobotic work cells that utilize methods from traditional robotic manufacturing [3-16]. Visual feedback techniques may be well suited to the assembly of MEMS components in which small lot sizes and diverse parts makes traditional fixturing infeasible [8]. Systems that rely on visual feedback alone can suffer from the limited depth perception available when viewing images at high magnification [8,12,13,15]. Advanced vision techniques, such as “depth from focus” use a series of 2-D images to produce a 3-D map of the work area, and have improved assembly procedures [15,17-19]. However, even with these improvements, visual feedback can be rather costly, slow and require an elaborate equipment setup. Additionally, the view may become obstructed by the work tool or assembly component during complex assemblies [12]. The integration of force feedback into microgrippers and tweezers for pick and place operations has led to improvements in yield and reliability [9,11,12,14-16]. Similarly, the incorporation of force feedback information from parts interactions during the assembly process will lead to more reliable and robust assembled devices [13-16].

One classical application for assembly is for pin-in-the-hole operations. This simple problem of inserting a pin or shaft into a hole accurately depicts many real-world assembly

Copyright © 2005 by ASME

tasks and can be used to characterize an assembly method. Whitney outlines the forces and reactions experienced during this type of assembly task that can be characterized by a force in the z-direction, and moments about the x and y axes [20]. Typical reaction forces produced during microassembly can range from mN to μN [7].

There are currently few, if any, commercially available force transducers that can meet the needs of such microassembly operations. For example, the Nano-17 force transducer from ATI Industrial Automation can measure forces in the range of ±17 N with a resolution of 12.5 mN [21].

Previous researchers have developed force transducers that are often very specific to one application and may lack the versatility to be used for other purposes. Sun *et al.* [22] developed a device to sense forces in the x and y directions with resolutions less than 1 μN. This device used capacitive comb drives. While the resolution for the device is very good, the current comb drive configuration may not be able to accommodate larger ranges of forces while maintaining this level of resolution. Other researchers have explored piezoresistive sensors for small force applications [12, 14, 16, 23, 24]. Dao *et al.* [23, 24] developed a six-degree-of-freedom piezoresistive sensor with mN range. This sensor used a compliant platform approach with 16 embedded peizoresistors arranged in a half-active Wheatstone bridge fashion. This design is well suited for the microassembly applications discussed here. In this paper, the implementation of this design in a surface micromachined process is explored.

The objective of the research is to design and develop a surface micromachined force transducer that measures the force in the z-direction and moments about x and y axes. This transducer will need to detect loads in the mN range with resolution on the order of 10 μN. The proposed device incorporates piezoresistive sensing elements onto a multi-leg, compliant platform device, yielding a three degree of freedom force transducer. Because the piezoresistive effect is lower in polysilicon than in silicon, the challenge will be to create a design to compensate for this reduced sensitivity. Various configurations and sensor element layouts are explored to determine the relationship of the applied forces and moments experienced during assembly and the corresponding strain. This paper presents the supporting theory and proof-of-concept for the resulting micromachined devices.

NOMENCLATURE

δ_R , ratio of change in resistance to nominal resistance
ΔR, change in resistance
R, nominal resistance
G, piezoresistive gauge factor
ε , strain
V_o , output voltage
V , applied voltage
δ , displacement of cantilever beam
P, measured load
l , half length of beam
E , Young's Modulus
I , moment of inertia
S_{max} , maximum stress
h , thickness of beam
d , displacement of fixed-guided beam
L , length of beam
F_z , measured force in z
M_i , moment about i, where i = x, y
V_i , voltage from signal i, where i = 1,2,3
$\overline{T}$, transformation matrix
$\overline{C}$, calibration matrix
$\overline{L}$, load matrix

SENSING MECHANISM

There are two sensing methods that are most often employed in micromachined sensors: capacitive sensing and piezoresistive sensing. Of these methods, capacitive sensing provides high resolutions but can require complex circuitry to process the signal, especially for multi-axis applications. Alternatively, piezoresistive sensing is easy to implement and can even be accomplished without the use of a complimentary metal-oxide semiconductor (CMOS) process. Piezoresistive methods have also been proven viable as shown by Stalford *et al*. [25], who demonstrated the use of piezoresistive sensing created entirely within a modified SUMMiT fabrication process. Drawbacks to piezoresistive sensing include a large area needed for the resistor elements and piezoresistive sensing can be time dependent. For the application in this paper, the sensor design is sufficiently large that the physical size of the resistor is not a limiting factor.

Piezoresistive materials have an electrical resistance that varies when placed under mechanical strain. This relationship can be treated as linear for small strains. The ratio, δ_R, of the change in resistance, ΔR, to the nominal resistance, R, is given as

$$\delta_R = \frac{\Delta R}{R} = G\varepsilon \tag{1}$$

where G is the gauge factor of the material and ε is the strain [26]. An advantage of using piezoresistive sensing is that the signal detection can be accomplished using a Wheatstone bridge circuit. Figure 1(a) shows a single-active Wheatstone bridge and Figure 1(b) shows a half-active bridge.

For the single-active Wheatstone bridge, only one resistor experiences the mechanical strain. Assuming all resistors have the same nominal resistance value, R, the relationship between the applied voltage, V, and the output voltage, V_o, is given as

$$\frac{V_o}{V} = \left(\frac{1}{2} - \frac{R(1+\delta_R)}{R + R(1+\delta_R)}\right) \tag{2}$$

With the assumption that δ_R is a very small number, this further reduces to

$$\frac{V_o}{V} \approx \frac{\delta_R}{4}. \tag{3}$$

Copyright © 2005 by ASME

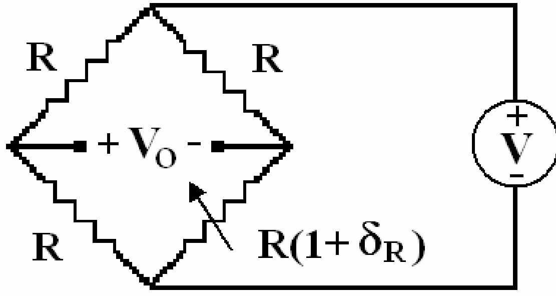

(a)

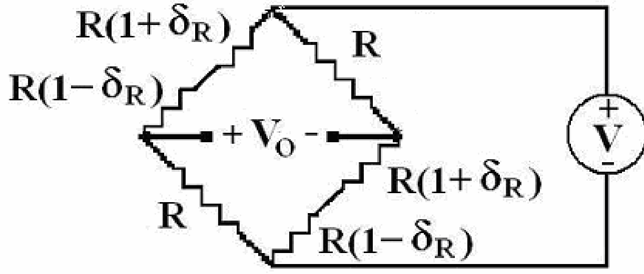

(b)

Figure 1. Wheatstone bridge diagrams: (a) Single-active and (b) Half-active Wheatstone bridge circuits.

For the half-active Wheatstone bridge, the voltage relationship is given as [24]

$$V_{out,Fz} = 0.25\left(\frac{\Delta R_{Fz1} + \Delta R_{Fz4}}{R_{Fz1} + R_{Fz4}} - \frac{\Delta R_{Fz2} + \Delta R_{Fz3}}{R_{Fz2} + R_{Fz3}}\right)V_{in}. \quad (4)$$

$$V_{out,Mx} = 0.25\left(\frac{\Delta R_{Mx1} + \Delta R_{Mx3}}{R_{Mx1} + R_{Mx3}} - \frac{\Delta R_{Mx2} + \Delta R_{Mx4}}{R_{Mx2} + R_{Mx4}}\right)V_{in}. \quad (5)$$

A half-active bridge configuration has higher sensitivity and linear output. In this configuration, it is necessary that the magnitudes of the change in resistance for the two active elements are well matched; therefore the location of the resistors is crucial. Also, this configuration provides thermal compensation [24]. Designs presented below incorporate resistor placements for both single-active and half-active Wheatstone bridges.

Because the deflection of the beams is small as compared to the length of the legs, linear beam theory may be employed to determine a relationship between the applied load and the strain. Assuming fixed-guided boundary conditions for each leg, the deflection at the midpoint of the leg is found using equations 6, per reference [27].

$$\delta = \frac{Pl^3}{3EI} \quad (6)$$

where P is the leg's share of half the load applied to the platform, l is half the length of the leg, E is the Young's modulus and I is the area moment of inertia of the cross section of the leg. Using symmetry, the displacement, d, at the end of the leg can found by multiplying δ by a factor of 2. The maximum stress in the leg can be computed using equation 7 [27].

$$S_{\max} = \frac{3Eh}{L^2}d \quad (7)$$

The entire length the beam is represented by L, and the thickness of the cross section by h. See Figure 2 for a two leg diagram.

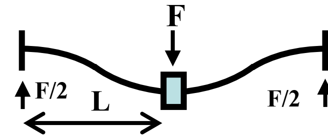

(a)

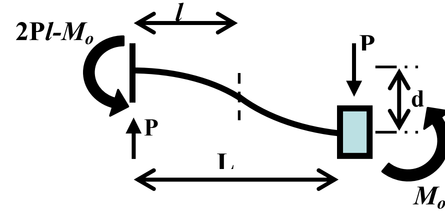

(b)

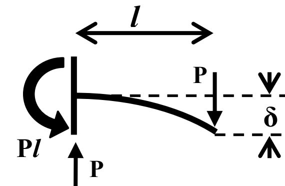

(c)

Figure 2. Free-body diagrams for (a) Two legs supporting a platform, (b) A fixed-guided flexible leg segment, and (c) Vertically end-loaded cantilever beam.

FABRICATION PROCESS

In this paper, the proposed device is planar. Hence, the fabrication appears to be simple and there are several methods that may be appropriate. The fabrication method must allow the use of a piezoresistive material with a sufficiently large gauge factor, such as silicon or polysilicon. The process must also allow for the finished device to move freely within its workspace and have electrical isolation between the resistor material and the structural material.

One possible method is to use the standard SUMMiT process with a backside Bosch etch [28], shown in Figure 3. This would require using the substrate silicon as the structural layer, silicon nitride as the electrical isolation layer and

Copyright © 2005 by ASME

creating the piezoresistors in the 0.3 μm polysilicon layer. Then, following the standard SUMMiT release, a two level mask backside etch can be performed to fully release the structure, as in Figures 3(d) and 3(e). The alignment tolerance between front side deposition and backside etching is ± 5μm.

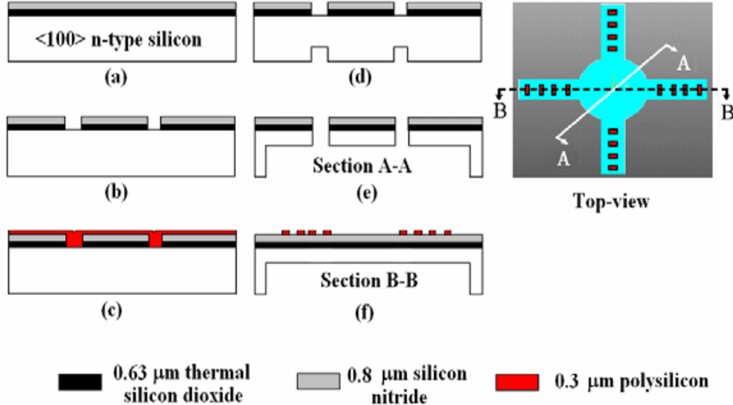

Figure 3. Cross-section view of fabrication method showing deposition of polysilicon resistors and backside etch.

DESIGN LAYOUTS

The proposed design uses piezoresistive strain gauges to determine an applied force. The device consists of a central platform supported by flexible legs. As a force is applied to the platform, the deflection of the legs will induce strain in the piezoresistors. Two platform designs are considered, a four-leg and three-leg configuration. Both configurations are shown in Figures 4 (a) and 4 (b). In addition, there are several possible layouts for the resistor elements; two layouts are presented here.

Single-Active Resistor Layout

One possible layout for this device is a platform design in which resistors are placed at the fixed end of the legs, in an area that will experience maximum strain when a load is applied. This can be accomplished using any number of legs, with three being the minimum for stability and signal conditioning. Designs with either three or four legs are considered here. Resistor placement for a four-leg design is shown schematically in Figure 5(a). Each leg has one sensing element that is connected to a single-active bridge. The force (F_Z) and moments (M_X, M_Y) can be determined from the output voltages (V_i, for sensor element i) using a transformation matrix, e.g., for the three-leg configuration

$$\begin{Bmatrix} F_Z \\ M_X \\ M_Y \end{Bmatrix} = \begin{bmatrix} T_{11} & T_{12} & T_{13} \\ T_{21} & T_{22} & T_{23} \\ T_{31} & T_{32} & T_{33} \end{bmatrix} \begin{Bmatrix} V_1 \\ V_2 \\ V_3 \end{Bmatrix} = \overline{T}\overline{V} . \tag{8}$$

The transformation equation for the four-leg configuration is as follows

$$\begin{Bmatrix} F_Z \\ M_X \\ M_Y \end{Bmatrix} = \begin{bmatrix} T_{11} & T_{12} & T_{13} & T_{14} \\ T_{21} & T_{22} & T_{23} & T_{24} \\ T_{31} & T_{32} & T_{33} & T_{34} \end{bmatrix} \begin{Bmatrix} V_1 \\ V_2 \\ V_3 \\ V_4 \end{Bmatrix} . \tag{9}$$

In order to determine the transformation matrix $\overline{T}$, it is convenient to define a calibration matrix $\overline{C}$ that transforms force and moments into voltage. Analogous to reference [6], the elements of the calibration matrix can be determined using

$$\overline{C} = \overline{T}^{-1} = \overline{V} \cdot \overline{L}^T \cdot (\overline{L} \cdot \overline{L}^T)^{-1} . \tag{10}$$

The $\overline{L}$ matrix is made up of applied loads, $\bar{l}_1$, $\bar{l}_2$,…, $\bar{l}_n$ where n must be greater than three and the $\overline{V}$ matrix is made up of the corresponding output voltages. The transformation and calibration matrix are related through the inverse. For the three-leg configuration the transformation matrix is square. Thus, the calibration for the three-leg case is mathematically simpler than the four-leg configuration that yields a non-

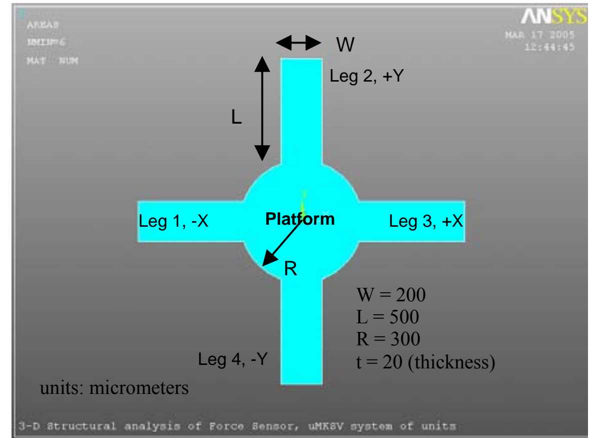

(a)

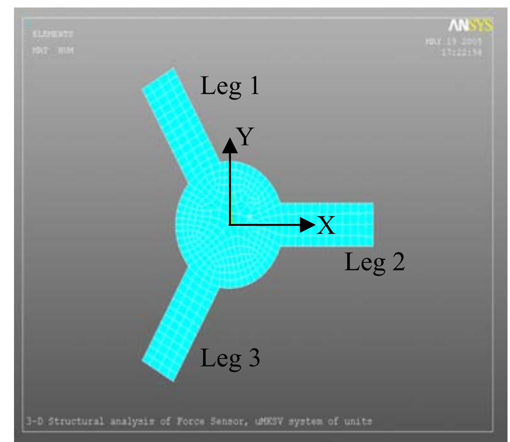

(b)

Figure 4. Schematics of transducer configurations: (a) Four-leg design and (b) Three-leg design.

Copyright © 2005 by ASME

square matrix. To address the issue of the non-square matrix, another resistor layout is proposed for the four-leg configuration.

Half-Active Resistor Layout

The second resistor design uses multiple sensing elements on each leg and connects them to form three half-active Wheatstone bridges, one for each force and moment direction of interest. These three Wheatstone bridges share a common half bridge, in which the resistors used for sensing are arranged at points along the legs (refer to Figure 5(b)). The two resistors in the common half bridge will be equal and experience no change in resistance when loads are applied. The M_{Yi} corresponds to resistor i (sensing element i) of the Wheatstone bridge for measuring moments about the y axis, and so forth.

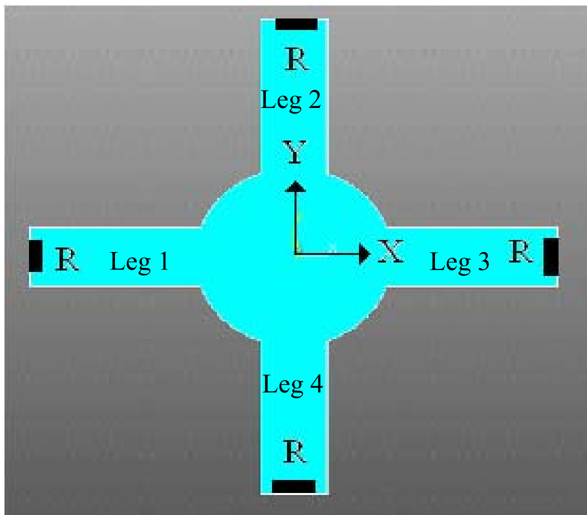

(a)

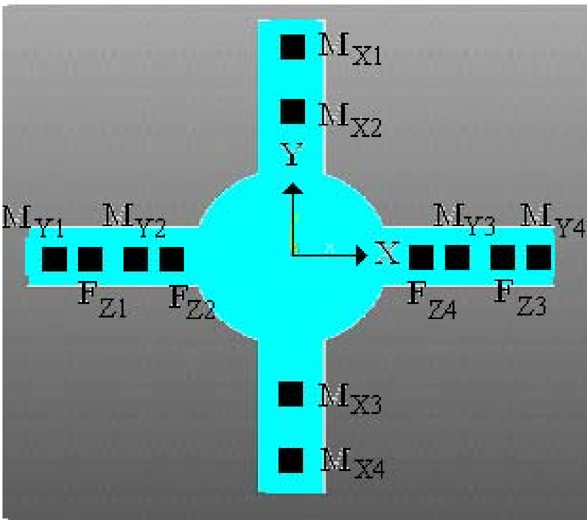

(b)

Figure 5. Resistor configurations for a four leg platform based force transducer: (a) One resister (sensor element) per leg – single-active Wheatstone bridges per leg layout, and (b) Resistor layout using three half-active Wheatstone bridges.

PIEZORESISTIVE CHARACTERIZATION

In order to predict the output from the piezoresistive sensors fabricated in SUMMiT V, it is necessary to have an estimate for the gauge factor of the polysilicon. Some reference materials will cite that polysilicon has a gauge factor of 50, about half that of single-crystal silicon. These same references will also acknowledge that the gauge factor of polysilicon is highly dependent on a number of factors, including doping level, grain size, and deposition conditions [26]. Therefore, it is necessary to determine a gauge factor for the first layer of polysilicon in the SUMMiT V process. Test structures have been fabricated for this purpose.

The test structures are 0.8 micron thick silicon nitride cantilever beams with 0.3 micron thick polysilicon resistors deposited at the fixed end. The beams, pictured in Figure 6, are 200x50 micrometers and are free to move from the substrate. The sensing resistor is connected in a single active Wheatstone bridge. As the beam is manually deflected in the positive z direction (away from the substrate), the change in voltage from the bridge is detected. The out-of-plane deflection is measured with an interferometer. Using beam mechanics, this measured deflection is related to the strain, which is used to determine an approximate gauge factor for the piezoresistors. An image of a deflected beam under the interferometer is shown in Figure 7. These experiments show the polysilicon piezoresistors to have a gauge factor of 24.88. This value can be used in conjunction with the force-strain information from finite element analysis (FEA) to determine the predicted voltage output and sensitivities for the force sensor designs.

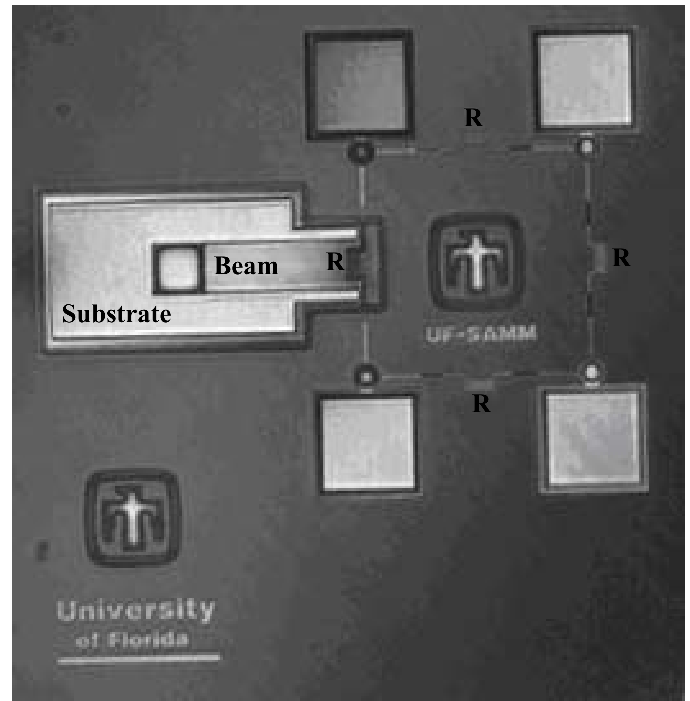

Figure 6. Micrograph of piezoresistive test structure in a single-active Wheatstone bridge.

Copyright © 2005 by ASME

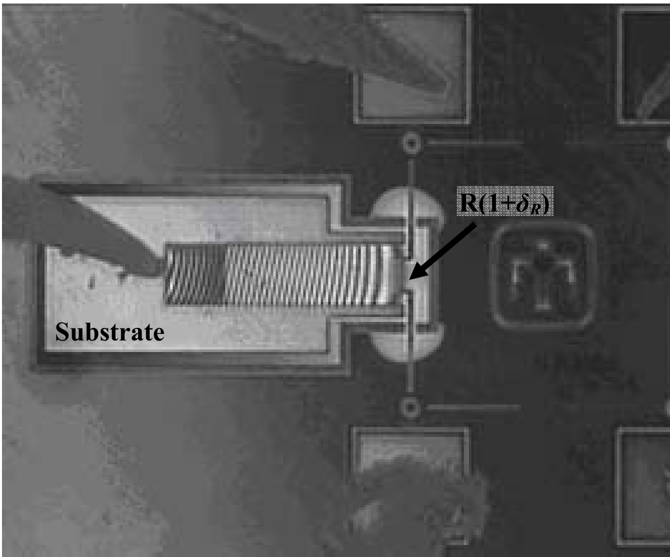

Figure 7. Interferometric image of out of plane deflection in the piezoresistive test structure.

RESULTS

An ANSYS FEA model of each device configuration and resistor layout is used to determine the stress response in the material for applied loads. Sample results for the four leg configuration subjected to a load in the z direction applied at the center of the platform are shown in Figure 8. From this and other loading cases, the two resistor layouts (single-active and half-active) can be evaluated to determine which design yields the best sensitivity.

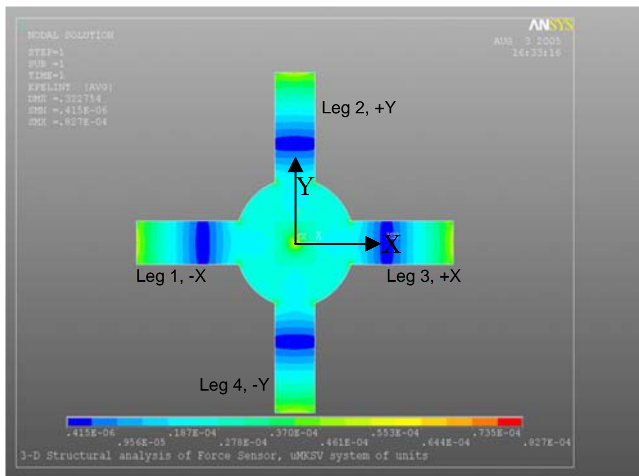

Figure 8. Graphical results of ANSYS simulation showing strain (microstrain).

Single-Active Resistor Layout

The sensitivity of the four-leg device using the first resistor layout was determined by applying a load from 0 to 1 mN at the center of the platform, perpendicular to the surface. The corresponding strains were calculated at the end of each leg. Using equation 3, with an input voltage of 5 volts, the output voltage was calculated. The results are shown in Figure 9.

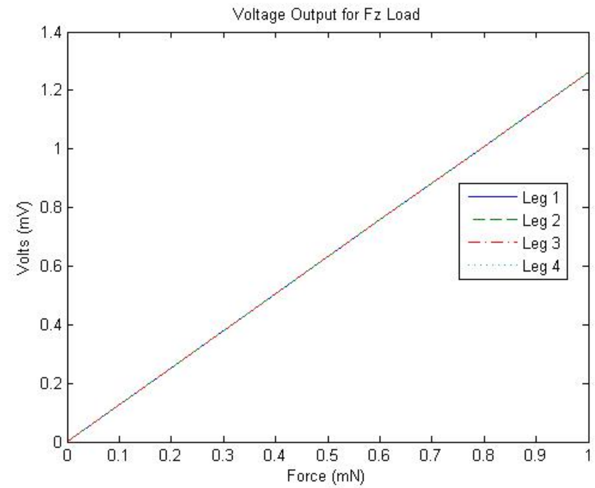

Figure 9. Voltage output for the single-active layout, four-leg configuration under loading in F_z.

Each leg shows an equal and linear response. Using the slope of the line, the sensitivity is found to be 1.26 mV/mN (0.252 mV_{out}/V_{in} for a 1 mN load). The voltage output corresponding to a loading in F_z in the range of 0 to 100 mN will be 0 to 126 mV. Assuming a sufficiently low signal-to-noise ratio, the minimum detectable voltage using a 12-bit analog to digital converter is 0.081 mV.

The same load conditions applied to the three-leg configuration using a single-active resistor layout resulted in a theoretical sensitivity of 2.06 mV/mN (0.412 mV_{out}/V_{in} for a 1 mN load). For measurements up to 100 mN, the voltage output is 0 to 206 mV. This corresponds to a minimum detectable voltage 0.10 mV of using a 12-bit analog to digital converter.

The symmetry of the four leg configuration causes the results for an applied moment about either the x- or y-axes to yield similar responses. Referring to Figure 5(a), a moment about the x-axis will be detected by the sensor elements in legs 2 and 4. Likewise, a moment about the y-axis will be detected in legs 1 and 3. Figure 10 shows the results for a positive moment applied about the y-axis with a magnitude of 0.15 μ(N-m). The sensitivity is 2.70 mV/μ(N-m) (0.54 mV_{out}/V_{in} for a moment of 0.15 μ(N-m)).

A positive moment about the y-axis with a magnitude of 0.15 μ(N-m) was applied to the three-leg platform. As expected, legs 1 and 3 show a similar response due to their symmetry about the x-axis. Similarly, a moment was generated about the x-axis with a magnitude of 0.15 μ(N-m) for the three-leg configuration. The resulting sensitivities to moments about the x- and y-axes are 16.7 mV/μ(N-m) (3.34 mV_{out}/V_{in} for a moment of 0.15 μ(N-m)), and 20 mV/μ(N-m) (4 mV_{out}/V_{in} for a moment of 0.15 μ(N-m)), respectively.

Half-Active Resistor Layout

To determine the sensitivity of the device using the second resistor layout, strain values are taken at locations along the length of the beam that correspond to the locations of the sensing elements. The same loading conditions for force and moments are applied for this device model. The response for a 1 mN load in the z-direction is shown in Figure 11.

 Copyright © 2005 by ASME

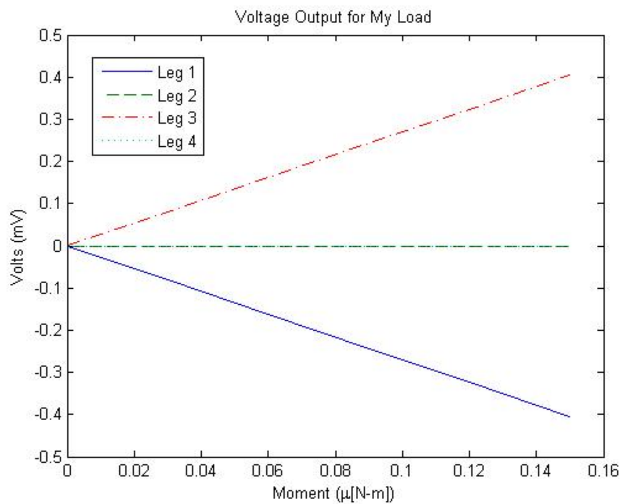

Figure 10. Voltage output for the single-active resistor layout in a four-leg configuration subjected to a moment about the y-axis.

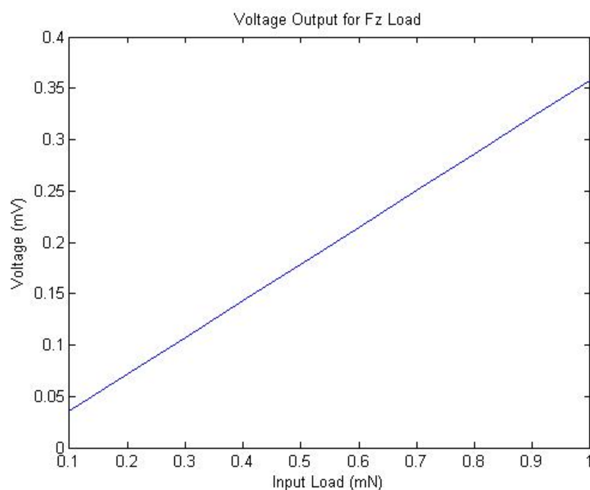

Figure 11. Voltage output for the F_z resistors, normal load.

The sensitivity for a normal load is 0.385 mV/mN (0.077 mV_{out}/V_{in} for a 1 mN load). The same resistors subjected to a moment of 0.15 μ(N-m) about the y-axis give a zero voltage output indicating that the output from the F_z sensing bridge will not be affected by a moment loading about either the x- or y-axes. The output of the sensing bridge for moment about the y-axis under a 0.15 μ(N-m) load is shown in Figure 12. The sensitivity for moment loads is 2.06 mV/μ(N-m) (0.412 mV_{out}/V_{in} for a 0.15 μ(N-m) load). Just as the F_z sensing was unaffected by a moment loading, the response of the M_y sensors from a normal load is also zero. The results for a moment about the x-axis are identical to those for the y-axis. This lack of cross talk between the different sensing bridges suggests that three desired degrees of freedom, F_z, M_x, M_y, can theoretically be detected and measured individually using the second resistor layout.

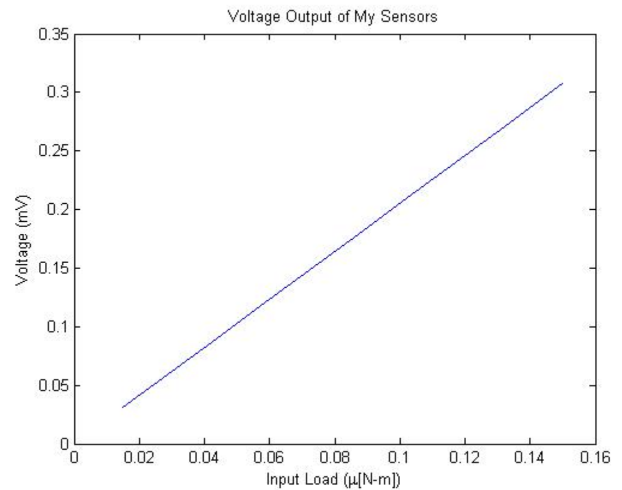

Figure 12. Voltage output for the M_y resistors, moment load.

As discussed in the details of the fabrication process, the alignment tolerance between front side resistor fabrication and backside etching is ±5 μm. It is important to understand how a misalignment of this magnitude can affect the output from the Wheatstone bridges in each design. A study of the change in strain resulting within this misalignment tolerance is presented for both resistor layouts. The strain induced by a normal load was measured a distance of 5 μm in both directions away from the resistor location parallel to the x-axis and y-axis. For the single-active resistor layout, the results show a less than 1% change in strain along the width of the leg. Along the length of the beam there occurs a 2.5% change in strain from the desired resistor location. The 2.5% change in strain reduced the sensitivity to normal loads from 1.26 mV/mN to 1.23 mV/mN. The half-active resistor layout saw the same change in strain along the y-direction, less than 1%. The maximum change in strain along the x-direction that occurred for any resistor location is 5.2%. Introducing these readings into the simulation changed the sensitivity to normal loads by 0.5%.

SUMMARY AND CONCLUSIONS

The work presented here discusses the major design issues for a three-axis micromachined force transducer with sensing abilities to meet the needs of microassembly tasks. Two resistor layouts were proposed that are based on the same planar platform structure. The first layout sensors arranged at the fixed ends of the legs as elements in single-active Wheatstone bridges. A calibration matrix is used to decouple and transform the readings into force and moment measurements. The second design uses 12 resistors located at various points along the length of the legs to determine the force and moments directly. These resistors are arranged into three half-active Wheatstone bridges. Structural analysis performed using finite element simulation is used to evaluate the suitability of each design.

At this early design stage, it appears that the single-active resistor layout yields the highest sensitivity. The resulting sensitivity for the four-leg platform is 1.26 mV/mN for forces in the z-direction. This resistor layout was also implemented on a three-leg platform providing a sensitivity of 2.06

Copyright © 2005 by ASME

mV/mN. The three-leg platform shows a higher sensitivity and will require less computation to calibrate due to the square transformation matrix. The higher sensitivity is a result of using fewer legs to support the same load as four legs. Therefore each leg will see a higher magnitude of strain and produce a stronger signal. Complex strains appear at the fixed end of the leg, where the resistors are located in the first layout. These undesirable stress components may reduce the sensitivity or provide inaccurate readings.

The sensitivities of the half-active resistor layout for normal and moment loads are 0.385 mV/mN and 2.06 mV/μ(N-m), respectively. The lower sensitivities may be corrected by optimizing the device parameters. An advantage of this design is that the strain being detected by the resistors is more predictable and highly directional because the strain along to the length of the beam is much greater than the other components of strain at these locations, for the giving loading cases [23, 24].

Overall, the above sensitivities are off from the desired goal by a factor of 5 to 20 depending on which of the above configurations and layouts is chosen. However, the designs show promise especially considering there was no optimization performed in the above work. Thus, future work includes optimization of the model and a more in-depth parametric study to further improve the performance of the device. Analysis of noise and signal conditioning is required to ensure that the operation of the device will meet resolution requirements for microassembly tasks. After the sensitivity goals have been met, fabrication and calibration of the sensor design will begin. In addition, more complex three-dimensional designs are being considered that can offer a wider range of applications.

ACKNOWLEDGMENTS

Funding for this work is provided by the College of Engineering and Department of Mechanical and Aerospace Engineering of the University of Florida, a Graduate Engineering Minority (GEM) Fellowship, and a Sandia National Laboratories Campus Executive Fellowship.

This work was also supported by the United States Department of Energy under Contract DE-AC04-94AL85000. Sandia is a multiprogram laboratory operated by Sandia Corporation, a Lockheed Martin Company, for the United States Department of Energy.

REFERENCES

[1] Bustillo, J.M., Howe, R.T, and Muller, R.S., “Surface Micromachining for Microelectromechanical Systems”, Proceedings of the IEEE, Vol. 86, No. 8, August 1998, pp. 1552-1574.

[2] Kovacs, G.T, Maluf, N.I., and Petersen, K.E, “Bulk Micromachining of Silicon”, Proceedings of the IEEE, Vol. 86, No. 8, August 1998, pp. 1536-1551.

[3] A. Rogner, J. Eicher, D. Munchmeyer, R. Peters, and J. Mohr, “The LIGA Technique— What are the New Opportunites”, Journal of Micromechanics and Microengineering, Vol. 2, pp.133–140, 1992.

[4] W. Menz, “LIGA and Related Technologies for Industrial Application”, Sensors Actuators A, Vol. 54, pp. 785–789, 1996.

[5] B.J Nelson, Y. Zhou and B. Vikramaditya, "Sensor-Based Microassembly of Hybrid MEMS Devices," *IEEE Control Systems*, Vol. 18, No. 6, pp. 35-45, Dec. 1998.

[6] S.E. Rose, J.F. Jones, and E.T. Enikov, “Development of a High Sensitivity Three-Axis Force/Torque Sensor for Microassembly”, Proceedings of ASME-IMECE, 2005.

[7] J.F. Jones, D.M. Kozlowski, and J.C. Trinkle, “Micro-scale Force-Fit Insertion”, Journal of Micromechanics, Vol. 2, No. 3-4, pp. 185-200, 2004.

[8] J.W. Feddema, and R.W. Simon, “Visual Servoing and CAD-driven Microassembly”, IEEE Robotics and Automation Magazine, pp. 18-24, December 1998.

[9] M.B. Cohn, K.F. Böhringer, J.M. Noworolski, A. Singh, C.G. Keller, K.Y. Goldberg, and R.T. Howe, “Microassembly Technologies for MEMS”, Proceedings of 1998 SPIE Conf. on Micromachining and Microfabrication Process Technology IV, Vol. 3511, pp. 2-16, Santa Clara, CA, Sept. 1998.

[10] A. Sulzmann, J.-M. Breguet, and J. Jacot, “Micromotor Assembly using High Accurate Optical Vision Feedback for Microrobot Relative 3D Displacement in Submicron Range”, IEEE International Conf. on Solid-State Sensors and Actuators, Transducers ’97, , pp. 279-282, Chicagp, June 16-19, 1997.

[11] G. Yang, J.A. Gaines, and B.J Nelson, “A Flexible Experimental Workcell for Efficient and Reliable Wafer-Level 3D Microassembly”, Proceedings of the IEEE International Conference on Robotics and Automation, Seoul, Korea, pp. 133-138, May 21-26, 2001.

[12] H. Van Brussel, J. Peirs, D. Reynaerts, A. Delchambre, G. Reinhart, N. Roth, M. Weck, and E. Zussman, “Assembly of Microsystems”, Annals of the CIRP, Vol. 49, No. 2, pp. 451-472. 2000.

[13] S. Fahlbusch, and S. Fatikow, “Force Sensing in Microrobotic Systems – An Overview”, Proceedings of the IEEE International conference on Electronis, Ciruits and Systems, pp. 259-262, 1998.

[14] S. Fahlbusch, and S. Fatikow, “Implementation of Self-Sensing SPM Cantilevers for Nano-Force Measurement in Microrobotics”, Ultramicroscopy, Vol. 86, pp. 181-190, 2001.

[15] S. Fatikow, J. Seyfried, S.T. Fahlbusch, A. Buerkle, and F. Schmoeckel, “A Flexible Microrobot-Based Microassembly Station”, Journal of Intelligent and Robotic Systems, Vol. 27, pp. 135-169, 2000.

[16] K. Domanaski, P. Janus, P. Grabiec, R. Perez, N. Chailet, S. Fahlbusch, A. Sill, S. Fatikow, “Design, Fabrication and Characterization of Force Sensors for Nanorobot”, Microelectronic Engineering, Vol. 78-79, pp. 171-177, 2005.

[17] J. Enns, and P. Lawrence, “An Investigation of Methods for Determining Depth from Focus”, IEEE Transactions on Pattern Analysis and Machine Intelligence, Vol. 15, No. 2, pp. 97-108, February, 1993.

[18] S.K. Nayar, and Y. Nakagawa, “Shape from Focus”, IEEE Transactions on Pattern Analysis and Machine Intelligence, Vol. 16, No. 8, pp. 824-831, March, 1994.

[19] M. Subbarao, and T. Choi, “Accurate Recovery of Three-Dimensional Shape from Image Focus”, IEEE Transactions on Pattern Analysis and Machine Intelligence, Vol. 17, No. 3, pp. 266-274, March, 1995.

Copyright © 2005 by ASME

[20] D.E. Whitney, “Quasi-Static Assembly of Compliantly Supported Rigid Parts”, Journal of Dynamic Systems, Measurement and Control, Vol. 104, pp. 65-77, March 1982.
[21] ATI Industrial Automation, http://www.ati-a.com/sensors .htm, February 21, 2005.
[22] Y. Sun, B.J. Nelson, D.P. Potasek, and E. Enikov, “A Bulk-Fabricated Multi-Axis Capacitive Cellular Force Sensor using Transverse Comb Drives.” J. Micromechanics and Microengineering, Vol. 12, pp. 832-840, 2002.
[23] D.V. Dao, T. Toriyama, J. Wells, and S. Sugiyama, “Six-Degree of Freedom Micro Force-Moment Sensor for Applications in Geophysics”, The 15th Annual IEEE Conference on MEMS, Las Vegas, NV, USA, pp. 312-315, Jan. 20, 2002.
[24] D.V. Dao, T. Toriyama, J. Wells, and S. Sugiyama, “Silicon Piezoresistive Six-Degree of Freedom Force-Moment Micro Sensor”, Sensors and Materials, Vol. 15, No. 3, pp. 113-135, 2002.
[25] H.L. Stalford, C. Apblett, S.S. Mani, W.K. Schubert, and M. Jenkins, “Sensitivity of Piezoresistive Readout Device for Microfabricated Acoustic Spectrum Analyzer,” Proc. of SPIE, vol. 5344, pp.36-43.
[26] S.D. Senturia, *Microsystem Design,* Kluwer Academic Publishers, Boston, MA, 2001.
[27] J.W. Wittwer, T. Gomm, and L.L. Howell, “Surface Micromachined Force Gauges: Uncertainty and Reliability”, J. of Micromechanics and Microengineering, Vol. 12, pp.13-20, 2002.
[28] Sandia National Laboratories, http://www.sandia.gov/ mstc/technologies/micromachines/techinfo/technologies/ summit5.html, February 10, 2005.

Copyright © 2005 by ASME